

## NUMERICAL SIMULATION OF THE DROPLET BREAKUP IN MICROCHANNELS WITH T-JUNCTION

Angel Edecio Malaguera Mora, [aemalagueram@gmail.com](mailto:aemalagueram@gmail.com)

Ana Lúcia. F. de Lima e Silva, [alfsilva@unifei.edu.br](mailto:alfsilva@unifei.edu.br)

Sandro M. M. de Lima e Silva, [metrevel@unifei.edu.br](mailto:metrevel@unifei.edu.br)

Federal University of Itajubá, Pinherinho, Itajubá, Postal 1303, Brazil

**Abstract.** *The influence of capillary number and the initial length of drops confined in microchannels on the mechanism of breakup is an important issue in the study of microfluidic. This paper describes numerically the droplets breakup in microchannels with T-junction. The simulations are done in a microchannel of 400 x 400  $\mu\text{m}$ , using two immiscible liquids. The simulations were performed with the open software OpenFOAM, in which the Volume of Fluid (VOF) method is implemented in interDyMFoam solver. To achieve a correct representation of the liquid/liquid interface the simulations were carried out using local grid refinement. Furthermore, the tool was used snappyHexmesh for greater refinement near the walls of the microchannel and thus to model the existing thin liquid layer formed between the droplet and the wall. The results show that the droplet breakup condition depends on the number of capillary and the initial length. According to the literature, it is possible to predict the droplet behavior after the junction as a function of the number of capillary and geometric dimensionless parameters. The results were in agreement with numerical data of the literature.*

**Keywords:** *Microfluidics, Volume of Fluid, interDyMFoam, Breakup mechanism, T-junction.*

### 1. INTRODUCTION

Two-phase flows in microchannels have recently attracted many researchers due to their wide applicability in modern and advanced technologies such as micro-electronics, chemical process engineering, genetic engineering, bioengineering, miniaturization of devices and other fields such as aerospace, chemical and nuclear industries. Heat exchangers implemented in equipment such as supercomputers, lasers and nuclear reactors are among the current applications (Park *et al.* 2008).

Several features of two-phase flows in microchannels have been investigated in recent decades, for example, two-phase flow patterns (Fukano, 1993 and Triplett, 1999a), the pressure drop (Triplett *et al.* 1999b) and the patterns of two-phase flows in parallel microchannels (Hetsroni *et al.* 2003). Numerical and experimental studies, on the dynamics of bubbles and droplets in microfluidic devices, have been performed by several researchers with the aim of studying the breakup and coalescence conditions (Fu *et al.* 2011; Afkhami *et al.* 2011 and Hoang *et al.*, 2013). The bubble dynamics is similar to that observed in drops flowing in microchannels, according to the literature (Jullien *et al.* 2009).

Recently, the technology in microfluidics flow has advanced as a new field of research. It provides a new approach, for example, to prepare and to control micro-dispersed emulsions, which have been widely used in chemical reactions, bioassays, separation processes and synthesis of materials. Monodisperse emulsions can be controllably prepared in microchannels with T-junctions with dimensions between 10 and 500 micrometers. The number of capillaries, which is the ratio between the viscous effects and surface tension forces, is the most important parameter in this study. Studies show that in microchannels with T-junction, the break/no-break conditions of drops and bubbles is mainly influenced by the number of capillary and the dimensionless width of the microchannel,  $l_o/w$  (Hoang *et al.* 2013).

Numerical simulations of two-phase flows in very small geometries are well known to be complex. Large capillary forces, combined with the effect of the confinement, takes to the breakup of drops and the mechanisms that cause separation are just a few examples of the complexity of this kind of simulation (Afkhami *et al.* 2011). Another difficulty encountered in this type of simulation is the high computational cost when using great mesh refinements in the computational domain in order to capture the flow details. The calculation of physical properties through the interface, such as density and viscosity is another difficulty encountered. A good representation of the interface implies a more accurate calculation of these properties. There are various techniques designed in order to overcome these drawbacks. One of the most popular techniques are the methods based on meshes with capture or tracking interface. Among them can be mentioned Front Tracking methods, Immersed Boundary, Volume of Fluid (VOF) and Level Set (LS).

The present study it is aimed to numerically study the breakup of drops in microchannels with T-junction using the open source software OpenFOAM and VOF methodology through the interDyMFoam solver that solves the equations for two-phase incompressible flows with dynamic mesh. To achieve a proper representation of the interface between the two fluids, the simulations were conducted using the dynamic local refinement.

## 2. MATHEMATICAL FORMULATION

In this work, the dynamics of a drop in a liquid moving inside a microchannel is studied. Both the continuous and dispersed phase are treated as incompressible fluids. The physical properties such as density and viscosity are constant in each phase, except on the interface. The Navier-Stokes equations in its conservative form can be written as follows:

$$\rho \left[ \frac{\partial \mathbf{U}}{\partial t} + \nabla \cdot (\mathbf{U} \times \mathbf{U}) \right] = -\nabla p + \nabla \cdot [\mu(\nabla \mathbf{U} + \nabla \mathbf{U}^T)] + \rho \mathbf{g} + \mathbf{F}_S \quad (1)$$

and conservation of mass by:

$$\nabla \cdot \mathbf{U} = 0 \quad (2)$$

where  $\mathbf{U}$  is the velocity vector of the fluid,  $p$  is the pressure,  $\mathbf{g}$  the gravity vector,  $\mathbf{F}_S$  is the interfacial force per unit volume acting on the interface between the two fluids and  $\rho$  and  $\mu$  are the density and viscosity, respectively.

The Navier-Stokes equations must be complemented by an equation that relates the deformations and tensions within the fluid. In this study, the fluids is Newtonian, thus the viscous stress tensor is given by:

$$\boldsymbol{\tau} = \mu(\nabla \mathbf{U} + \nabla \mathbf{U}^T) \quad (3)$$

In VOF methodology, the volume fraction is used as an indicator function (phase  $\alpha$ ) to mark the different fluids. The interface is defined as a transition region and is treated as a mixture two fluids. The volume fraction ( $\alpha$ ) is defined as the fraction of the volume of control occupied by one of the liquids ( $0 \leq \alpha \leq 1$ ), and it is used for following the interface moves. When  $\alpha = 1$ , the volume control contains only one phase (dispersed), and when  $\alpha = 0$ , the other phase (continuous). Using this definition of volume fraction, the density and viscosity can be represented as:

$$\rho(\mathbf{x}, t) = \alpha \rho_c + (1 - \alpha) \rho_d \quad (4)$$

$$\mu(\mathbf{x}, t) = \alpha \mu_c + (1 - \alpha) \mu_d \quad (5)$$

where the indices  $c$  and  $d$  are used to designate the dispersed and continuous phases, respectively. The transport equation for the function  $\alpha$  can be written as follows:

$$\frac{\partial(\alpha)}{\partial t} + \nabla \cdot (\mathbf{U}\alpha) = 0 \quad (6)$$

Equation (6) is the equation of advection or transport of the volume fraction that capture the interface that is moving. The unit vector normal to the interface is given by:

$$\mathbf{n} = \frac{\nabla \alpha}{|\nabla \alpha|} \quad (7)$$

The CSF model (Continuous Surface Force) is used to represent the interfacial force  $\mathbf{F}_S$  as a body force distributed along to the interface with a finite thickness, given by:

$$\mathbf{F}_S = \sigma k \mathbf{n} \delta(x) \quad (8)$$

where  $\sigma$  is the surface tension coefficient,  $k$  means the curvature of the interface and  $\delta(x)$  the delta Dirac function concentrated on the interface and zero in the other regions.

The interface is represented in the field with a finite thickness where the volume fraction varies smoothly from zero to one at a distance comparable with the spacing of an elementary volume of the mesh. Thus, the volumetric form  $\mathbf{F}_S$  is nonzero only within this transition region, and is given by:

$$\mathbf{F}_S(\mathbf{x}, t) = \sigma k(\mathbf{x}, t) \left[ \frac{\nabla \alpha}{|\nabla \alpha|} \right] \delta(x) \quad (9)$$

In VOF method, the interface is implicitly represented by the VOF function  $\alpha$ , whose values change over a thin region. This change may generate errors in the normal vector and curvature calculation. As consequence, the surface force will not be correctly evaluated and parasitic currents may rise in the interfacial region. Over the past decade, a number of researchers showed variations in CSF technique aiming to decrease the magnitude of parasitic currents. Early studies in

this direction are analyzed by Scardovelli and Zaleski (1999). Newer versions presented by Renardy and Renardy (2002) and Harvie et al. (2006).

### 3. DESCRIPTION OF THE NUMERICAL SIMULATION

The numerical codes are, undoubtedly, tools that provide great benefits and a greater ease in the analysis of different types of flow. Its importance has grown in recent years due to the reliability and speed with which results are obtained in addition to the economy in experimental tests. This is due to advances in the development of modeling of physical phenomena, the numerical techniques to solve problems and increased computing power. OpenFOAM was chosen to be used in this work because besides being free license software, it is also open source which allows the user to make new implementations if necessary. In addition, it is a robust code and provides quite reliable results for a range of practical problems.

The main objective of this work was the simulation of breaking drops in microchannels with T-junction. In these cases, it is important to accurately identify the drop border, which moves and deforms over time, within the microchannel. The correct representation of the interface is primarily needed at the instants at which rupture occurs or not, so the dynamic refinement technique implemented in *interDyMFoam* solver was used. Dynamic refinement is done where the  $\alpha$  function identifies the interface. This work defined a maximum number of refining cells around the interface 20,000,000.

OpenFOAM uses the Gauss integration with the Finite Volume method for the discretization of differential equations. This method is based on the sum of variable volume flows in the faces, which must be interpolated from the center of volume. The method adopted in these simulations for interpolation is the upwind scheme. For pressure-velocity coupling, PISO algorithm (Implicit Pressure with Splitting of Operators) was used. For the time integration, the explicit Euler scheme was used, controlling the passage of time with a maximum at 0.1 Courant. High number of Courant causes distortion in the interface due to the increase in parasitic currents (Hoang et al, 2013). In Section 4.1, the results of simulations of a case are presented to compare the effect of the number of Courant.

An initial computational domain was generated with hexahedral cells using the *blockMesh* tool. The grid near the walls of the microchannel is refined in order to model the thin liquid layer existing between the droplet and the wall. For this, the *snappyHexMesh* tool, which allows different levels of refinement, was used, as shown in Fig. 1. Note that there is major refinement at the junction and in direction  $x$ , i.e. with the intention of capturing greater detail during the drop break. As aforementioned, the dynamic refinement was carried out for all simulations in order to better represent the drop interface. Figure 1 illustrates, in section, the dynamic refinement generated on the interface with the *interDyMFoam* solver used in this work. This refinement is done in the areas of higher gradient of the volume fraction function,  $\alpha$ .

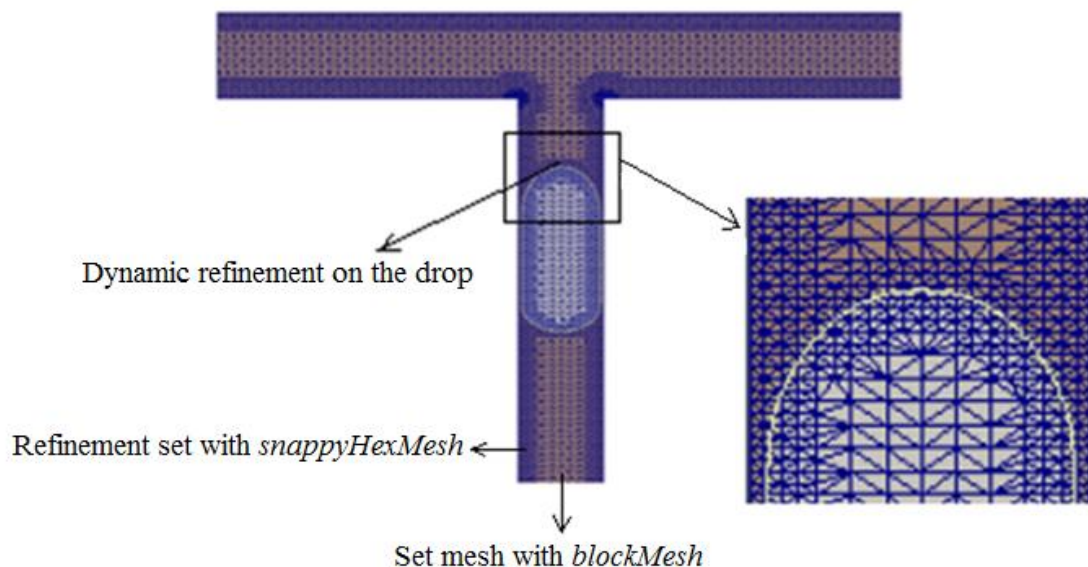


Figure 1. Computational domain generated the *blockMeshDict* file and *snappyHexMesh* tool, and the dynamic mesh of the drop interface generated by the solver *interDyMFoam*.

Figure 2 shows the important dimensions of the microchannel and drop. The transverse area of the microchannel ( $w$ ) was the same in all simulations ( $400 \times 400 \mu\text{m}$ ), and the length of the drop was established between ( $1,5 < l_o/w < 3,5$ ). This length  $l_o$  is measured when the drop arrives at the T-junction, which is determined during post processing. At the channel inlet, the drop has a greater length ( $L_o$ ). For all the simulations, the drop is initially a parallelepiped with a cross-section of  $300 \times 300 \mu\text{m}$ .

An initial velocity was established in each simulation for both dispersed (drop) and continuous (liquid in the channel) phases at the microchannel inlet and zero gradient condition for velocity on both walls. The condition of the walls of the microchannel was established as not sliding. A fixed value was established for the pressure in the output area.

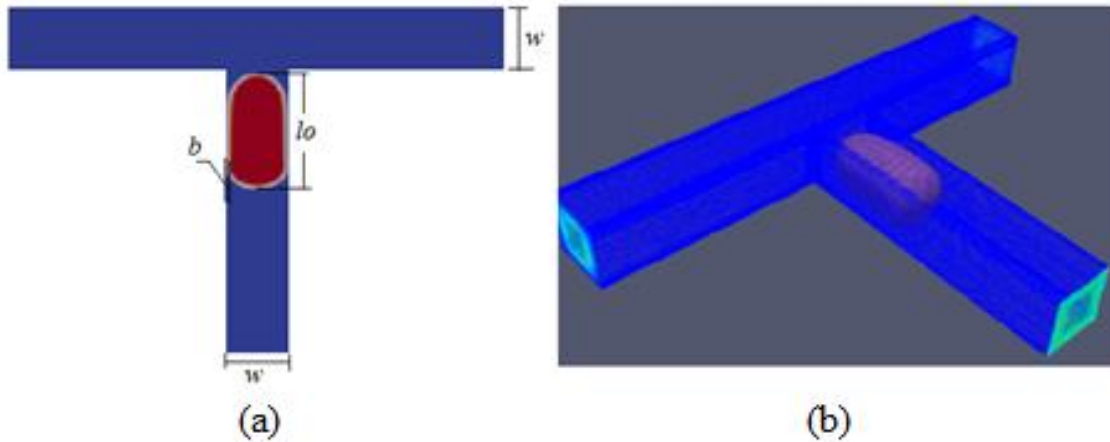


Figure 2. (a) Main dimensions of the computational domain and the drop, (b) Three dimensional view

The results reported by Fu et al. (2011) were used as an experimental basis and the results presented by Afkhami et al. (2011) and Hoang et al, 2013 were used for numerical comparison. These authors performed experimental and numerical studies respectively, to study the bubble break condition in microfluidic T-junction. In Hoang et al, 2013 the methodology implemented in VOF interFoam solver (without dynamic refinement) of OpenFOAM was also used.

The number of capillarity is a relationship between the effects of viscous forces and surface forces, where  $U_c$  is the speed of the continuous phase at the time that the drop is found in the T-junction and  $\eta_c$  and  $\sigma$  are respectively the viscosity and surface tension of the continuous phase. This parameter can be set by:

$$C_a = \frac{\eta_c U_c}{\sigma} \quad (10)$$

As already mentioned, the number of capillarity affects the breakup condition, and simulations with different values ( $0.01 \leq C_a \leq 0.12$ ) were performed for this analysis. This range of values was chosen according to literature results used for comparison. The rate of continuous phase when the drop enters the T-junction and the speed of the dispersed phase have been determined with the aid of Paraview post-processing program.

The fluid properties were determined in accordance with Hoang et al., 2013, and are shown in Tab. 1. For all simulations, an initial speed for the dispersed phase of 0.04 m / s was imposed, however the initial speed of the continuous phase was the variable selected in accordance with each simulated case.

Table 1. Fluid properties

Fluid	$\rho$ ( $kg/m^3$ )	$\mu$ ( $\frac{kg}{m \cdot s}$ )	$\sigma$ (N/m)
Continuous phase	770	$8 \times 10^{-3}$	0.005
Dispersed phase (drop)	1000	$1 \times 10^{-3}$	-

After solving the problem, the results were visualized on Paraview software. This tool allows the view of the mesh and geometry, the creation of 2D and 3D figures, generation of vector graphics, etc.

## 4. RESULTS

### 4.1 The influence of parasitic currents during the droplet breakup

The parasitic currents are nonphysical movements generated when using models such as the CSF techniques (Continuum Surface Force), to approximate the surface force calculation. Its magnitude generally increases as the surface force increases and may become so great that affects the prediction of the velocity field or in extreme circumstances may cause complete nonphysical disruption of the interface. These spurious currents are a major problem in the case of microfluidic due to the fact that they increase with the inverse of the capillary number but can be reduced in magnitude with the mesh refinement or by decreasing the time step.

Figure 3 shows the streamlines for two different simulations ( $C_o = 0.3$  and  $C_o = 0.1$ ) with a number of capillarity  $C_a = 0.08$  and  $l_o/w = 2.1$ . The results obtained with the small Courant number have small recirculation near the drop interface and the flow is asymmetric. These spurious currents increase the local velocity and they are responsible for the drop breakup and for its asymmetric shape.

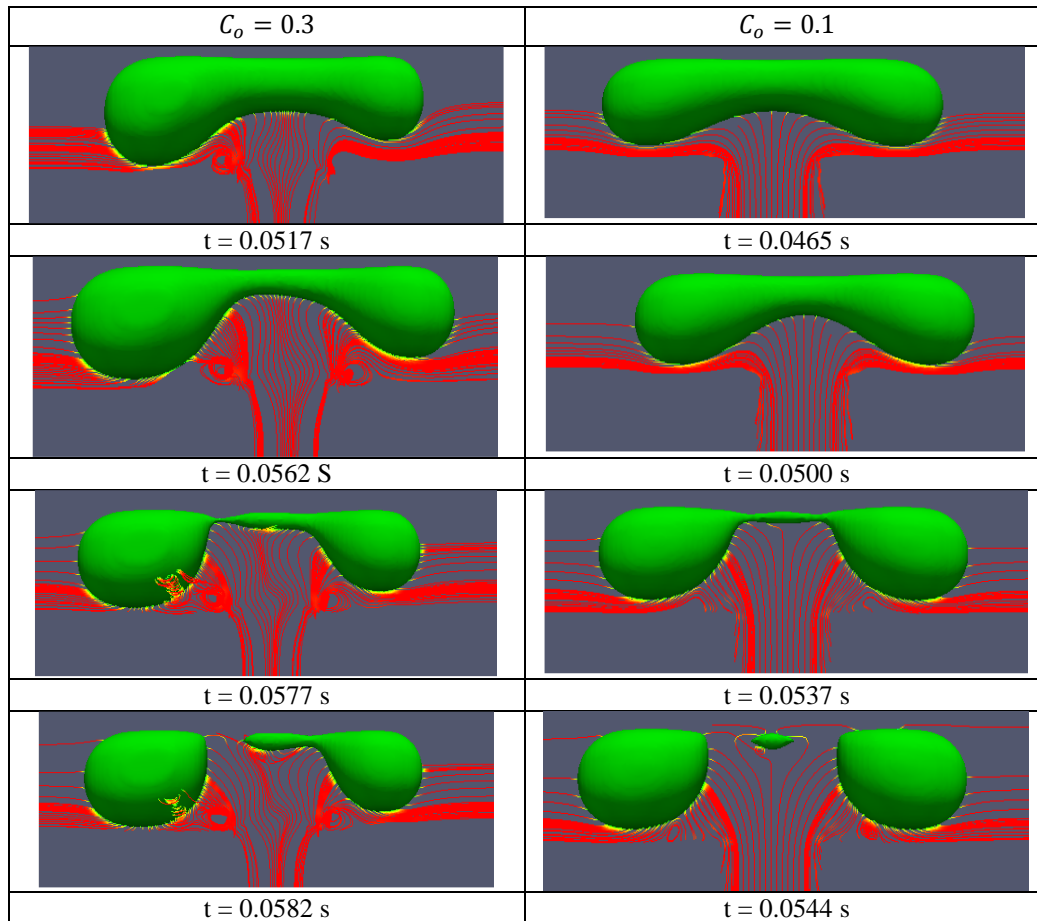


Figure 3. Temporal evolution of the drop compared during the break for Courant numbers 0.5 and 0.1 with  $C_a = 0,08$  and  $l_o/w = 2.1$ .

Figure 4 shows the velocity vectors for two simulations with different numbers of Courant. Two nearest possible time instants (0.0517 and 0.0465 s) were chosen so that the comparison could be made. In the case where the number of Courant was 0.3, a greater value of the speed in the lower region of the drop was observed. Furthermore, the obtained velocity field is asymmetric with respect to axis y. These higher speed values tend to compress the interface at the bottom of the drop, eventually producing its irregular breakage.

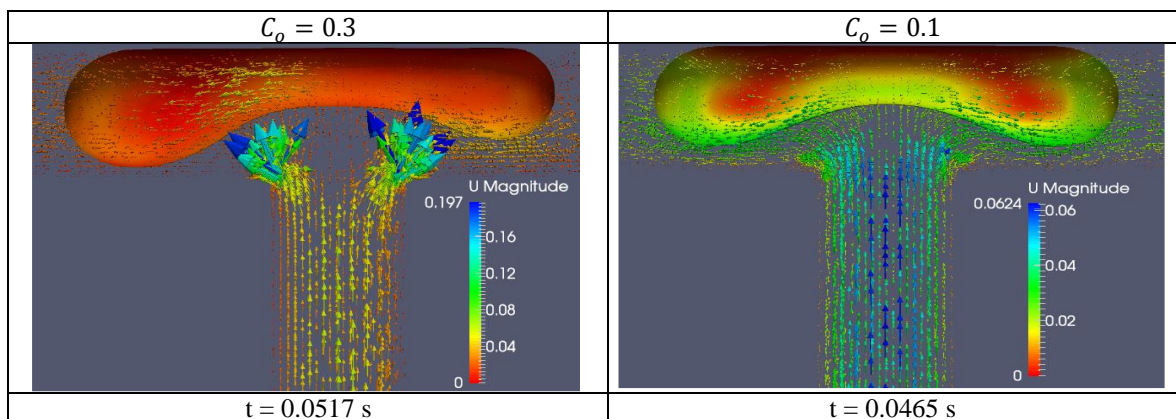


Figure 4. Velocity field on the drop simulated for Courant numbers 0.5 and 0.1 with  $C_a = 0.08$  and  $l_o/w = 2.1$ .

#### 4.2 Condition of breaking and non-breaking of the drops in T-junction.

The dynamics of small drops and bubbles flowing through T-junction is strongly influenced by the number of capillarity ( $Ca$ ) and the relationship between the length of the bubble ( $l_o$ ) and the width of the microchannel ( $w$ ), or ( $l_o/w$ ) at the time it arrives at the junction. Many numerical and experimental studies report phase diagrams of bubbles/drops expressed in terms of these two parameters showing when or not the breakup happens. At this stage we examine the VOF methodology implemented in OpenFOAM as the solver *interDyMFoam* to predict the breakup condition of the drop.

At the initial time, the droplet has a rectangular shape and the physical properties of the fluids are shown in Tab. 1. Initial drops were simulated in dimensionless length ( $l_o/w$ ) 2; 2.25; 2.5 and 3.5, and in all cases an initial speed was set for the dispersed phase ( $U_d$ ) 0.04 m/s. For the continuous phase, the initial velocity was the variable parameter of the simulation ( $0.01 < U_c < 0.05$  m/s). The capillarity number is calculated based on the properties of the continuous phase shown in Tab. 1 and based on the maximum speed at the moment when the droplet is completely within the bifurcation.

Figure 5 shows the results of this simulation and the results of the work of Afkhami et al. 2011 and Hoang et al. 2013. The green curve indicates the separation between breaking transition region and non-breaking proposed by Hoang et al. 2013. The results of the simulations in this work are shown with red and black triangles. The filled triangles represent the cases where there has been rupture and the empty ones for cases without rupture. The simulations of this work convey good agreement with the literature results.

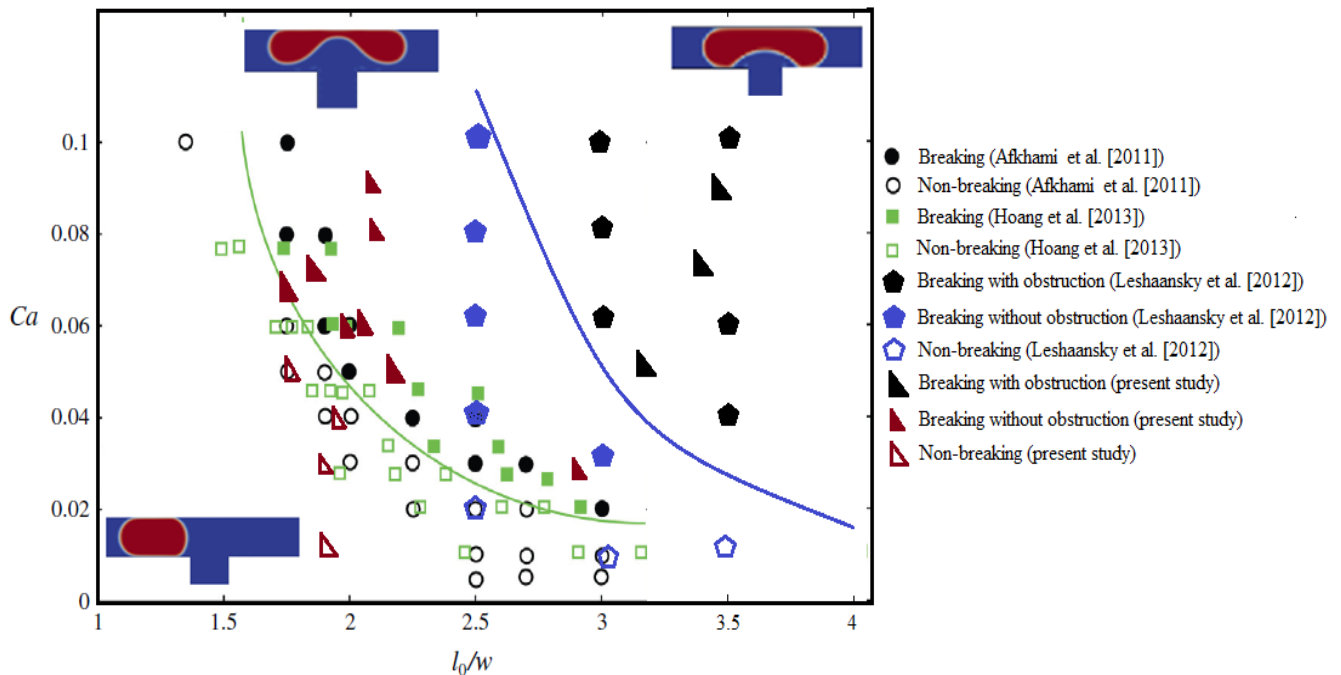


Figure 5. Phases diagram of numerical simulation for a drop in microchannels with T-junction.

The breaking mechanism can be presented in two ways: breaking with obstruction (or blocked) and breaking without obstruction. In the former case, space between the wall and the drop during the break is not observed visually. This behavior is generally for values of dimensionless length ( $l_o/w > 3$ ). In the no obstruction case, this distance between the wall and the drop is visible and a thin layer of liquid is observed. The black solid line indicates the transition between the two rupture regimes, that is, with and without obstruction as presented in the work by Leshansky et al. 2012. The simulations in this paper in the obstructed breakdown region show agreement with the results in literature.

The evolution of the smallest thickness of the drop,  $\delta/w$  in a previous moment to its break, for different cases was also analyzed. Several computational and experimental studies report the droplets or bubbles breaking mechanism in relation to these diagrams (Fu et al. 2011 and Jullien et al. 2009). The results are shown in Fig. 6 along with literature results. As shown in Fig. 6, the smallest thickness of the dimensionless drop decreases with time, as expected. In the simulated case, the drop break occurred at  $0.11 < \delta/w < 0.14$ . Moreover, both the influence of the capillarity number and the dimensionless length of the drop  $\delta/w$  are observed.

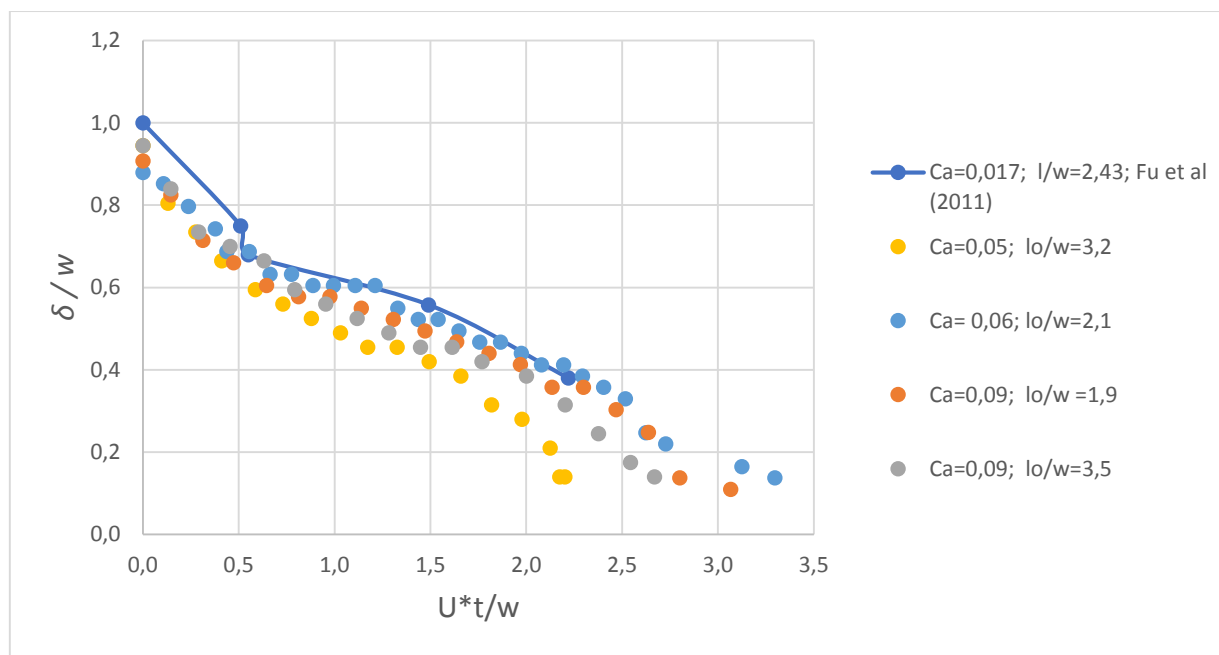


Figure 6. Temporal evolution of the neck width  $\delta$  for different droplet lengths and capillary number.

## 5. CONCLUSIONS

In this work, two-phase flow of a single drop in a liquid medium was simulated in a symmetrical microchannel with T-junction. The OpenFOAM program, which is based on the Volume of Fluid (VOF) methodology, was used. The drop initially had the shape of a parallelepiped and for all simulations its initial velocity was 0.04 m/s. This included the refinement layers, held near the walls of the channel (snappyHexMesh) and the dynamic refining performed on the droplet interface at each time instant. The bubble approached the junction with an approximately constant velocity, in accordance with the initial length chosen for the channel entrance. Upon arriving at the fork shape, it is elongated and displays rounded edges, featuring the so-called Taylor bubble. For both simulated cases, the burst and non-burst conditions were observed. The breaking / non-breaking condition depends on the number of capillarity and the drop length. Moreover, it was possible to identify the two break conditions with and without obstruction reported in literature. The breaking mechanism with obstruction occurred with dimensionless lengths of the drop greater than 2.5.

The parasitic or spurious currents that commonly appear in this type of simulation, based on VOF / CSF methodology, were controlled by reducing the number of Courant. These non-physical currents produce pressure on the interface, yielding non-symmetrical and non-physical breaking of the drop, as shown in this study.

## 6. ACKNOWLEDGEMENT

The authors acknowledge CAPES the Doctoral scholarship, CNPq, FAPEMIG and Mechanical Engineering Institute of UNIFEI for their support.

## 7. REFERENCES

- Afkhami, S., Leshansky, A. M. and Renardy, Y. 2011. "Numerical investigation of elongated drops in a microfluidic T-junction". *Physics of Fluids*. Vol. 23, 022002, pp.1-14
- Fu, T. Ma. Y., Funfschilling, D. and Li, H. Z. 2011. "Dynamics of bubble breakup in a microfluidic T-junction divergence". *Chemical Engineering Science*. Vol. 66, pp. 4184-4195.
- Fukano, T. and Kariyasaki, A. 1993. "Characteristics of gas-liquid two-phase flow in capillary tube". *Nuclear Engineering and Design*. Vol. 141, pp. 59-68.
- Harvie, D. J. E., Davidson, M. R. and Rudman, M. 2006. "An analysis of parasitic current generation in Volume of Fluid simulations". *Applied Mathematical Modelling*. Vol 30, pp. 1056-1066.

- Hetsroni, G., Mosyak, A., Segal, Z. and Pogrebnyak, E. 2003. "Two-phase flow patterns in parallel micro-channels". *International Journal of Multiphase Flow*, Vol.29, pp. 341-360.
- Hoang, D. A., Van Steijn, V., Portela, L. M., Kreutzer, M. T. and KLEIJN, C. R. 2013. "Benchmark numerical simulations of segmented two-phase flows in microchannels using the Volume of Fluid method". *Computers and Fluids*. Vol. 86, pp.28-36.
- Jullien, M. C., Tsang Mui Ching, M. J., Cohen, C., Menetrier, L. and Tabeling, P. 2009. "Droplet breakup in microfluidic T-junction at small capillary numbers". *Physics of Fluids*. Vol. 21, 072001 pp. 1-6.
- Leshansky, A. M., Afkhami, S., Jullien, M. C. and Tabeling, P. 2012. "Obstructed breakup of slender drops in a microfluidic T-junction". *Physical Review Letters*. Vol 108, 264502, pp 1-5.
- Park, H. S. and Punch, J. 2008. "Friction factor and heat transfer in multiple microchannels with uniform flow distribution". *International Journal of Heat and Mass Transfer*, Vol. 51, pp. 4535-4543.
- Renardy, Y. and Renardy, M. 2002. "PROST: A parabolic reconstruction of surface tension for the volume-of-fluid method". *Journal of Computational Physics*. Vol.183, pp. 400-421.
- Scardovelli, R. and Zaleski S, 1999. "Direct numerical simulation of free-surface and interfacial flow". *Annu. Rev. Fluid Mech*. Vol.31 pp. 567-603.
- Triplett, K. A., Ghiaasiaan, S. M., Abdel-Khalik, S. I. and Sadowski, D. L. 1999a. "Gas-liquid two-phase flow in microchannels. Part I: two-phase flow patterns". *International Journal of Multiphase Flow*, Vol.25, pp. 377-394.
- Triplett, K. A., Ghiaasiaan, S. M., Abdel-Khalik, S. I., Lemouel, A. and McCord, B. N. 1999b. "Gas-liquid two-phase flow in microchannels. Part II: void fraction and pressure drop". *International Journal of Multiphase Flow*, Vol.25, pp. 395-410.

## 8. RESPONSIBILITY NOTICE

The authors are the only responsible for the printed material included in this paper.